

Homofugality: A new reactivity index describing the leaving group ability in homolytic substitution reactions

Doris Guerra ^{a,*}, Raquel Castillo ^b, J. Andrés ^b, P. Fuentealba ^c,
A. Aizman ^d, R. Contreras ^{b,e}

^a *Departamento de Ciencias Químicas, Facultad de Ecología y Recursos Naturales, Universidad Andrés Bello, Av. República, 275, Santiago, Chile*

^b *Departament de Ciències Experimentals, Universitat Jaume I, Avda. Sos Baynat s/n 12006, Castelló, Spain*

^c *Departamento de Física, Facultad de Ciencias, Universidad de Chile, Casilla 653, Santiago, Chile*

^d *Departamento de Química, Universidad Federico Santa María, Casilla 110-V, Valparaíso, Chile*

^e *Departamento de Química, Facultad de Ciencias, Universidad de Chile, Casilla 653, Santiago, Chile*

Abstract

We propose and test a new reactivity index tentatively called homofugality, to quantitatively rank the leaving group ability of radical fragments present in homolytic substitution reactions. The model is validated for a series of S_H2 processes involving organometallic systems.

1. Introduction

The homolytic substitution reaction is a radical process that shares most of the mechanistic aspects of the analogous polar nucleophilic substitution, but at the same time it presents a significantly different range of applicability, in the sense that the attacked center can rarely be a carbon atom [1]. The bimolecular homolytic substitution (S_H2) may be a concerted process, in which a free radical R[•] forms a bond to A, with a simultaneous homolytic scission of the A–LG bond and loss of the radical LG[•], as shown below:



A parent class of reactions are the intramolecular homolytic substitutions (S_Hi), in which the attacking R[•] radical is tethered to the A–LG moiety of the molecule, so that the departure of the LG[•] radical is accompanied by ring formation. Stepwise routes for homolytic substitution reactions, involving the [R[•]··A··LG][•] intermediate have also

been proposed. Both the intermolecular and intramolecular homolytic substitution reactions have been reviewed by Ingold and Roberts [2], and more recently by Schiesser and Wild [3].

Despite the substantial potential that free radical attack at saturated carbon provides, particularly those leading to the formation of carbon–carbon bonds, there are relatively few examples of reactions of this type. The scarce kinetic data on these reactions involve activation of the carbon atom through strain or involvement of metal leaving group [1,4,5]. The absence of a complete body of kinetic data to describe the reactivity of the title reactions has significantly stimulated the theoretical calculation of reaction barriers and other properties of the ground and transition state structures on these systems. The free radical homolytic substitution reactions at Silicon, Germanium and Tin have received special attention from a computational point of view, and accurate activation barriers have been reported [6–8].

In this Letter we present a theoretical analysis of the S_H2 reactions involving silyl, germyl and stannyl radicals based on a set of global and local reactivity indices defined in the

* Corresponding author. Fax: +56 2 6618269.

E-mail address: do.guerra@uandresbello.edu (D. Guerra).

context of the spin polarized density functional theory [9–14]. A new descriptor of reactivity, the homofugality index defined as the group spin-philicity of the leaving group, is introduced and tested.

2. Model equations and computational details

The spin-philicity (ω_S^+) and spin-donicity (ω_S^-) indices have been introduced within the context of spin-polarized density functional theory (SP-DFT) by Contreras et al [12], to describe the stabilization in energy as the system exchanges spins with the environment in the direction of increasing (+) and decreasing (–) multiplicity. They have been given the following quantitative definitions:

$$\omega_S^+ \equiv -\frac{(\mu_S^+)^2}{2\eta_{SS}^0} \quad \text{and} \quad \omega_S^- \equiv -\frac{(\mu_S^-)^2}{2\eta_{SS}^0}. \quad (2)$$

μ_S^+ and μ_S^- are the spin potentials in the direction of increasing and decreasing multiplicity, respectively. η_{SS}^0 is the global spin hardness of the system. The spin-philicity (ω_S^+) and spin-donicity (ω_S^-) indices have been successfully applied to describe the spin catalytic activity of paramagnetic molecules [12]. Global spin philicity has been further applied to study spin polarization effects on the reactivity of carbenes, silylenes, germynes, and stannylenes [15] as well as simple nitrenes and phosphinidenes [16]. This concept has been recently generalized by Geerlings et al. to deal with the corresponding local counterpart [13], which has been defined as follows:

$$\omega_S^+(\mathbf{r}) = \omega_S^+ f_{SS}^+(\mathbf{r}) \quad (3)$$

where $f_{SS}^+(\mathbf{r})$ is the generalized spin Fukui function introduced by Galván et al. [9], as the derivative of the spin density with respect to the spin number $N_S = N_\alpha - N_\beta$. The local spin-philicity index is used here to define a new regional descriptor of reactivity, the homofugality index, which helps to categorize the leaving group ability of radical fragments in homolytic substitution reactions. We define the homofugality index (v^*) as the regional spin-philicity of the leaving group (LG) embedded in the substrate that undergoes a radical attack as follows:

$$v^* \equiv \omega_S^+(\text{LG}) = \sum_{k \in \text{LG}} \omega_{S,k}^+; \quad (4)$$

The quantity $\omega_{S,k}^+$ is a regional (condensed to atom) spin philicity. This definition requires that either, the leaving radical be involved in the rate determining step of a stepwise process or the presence of comparable bonding conditions in the bond forming process of a concerted pathway. In this work this second condition will be imposed to discuss the reliability of the homofugality index to describe the leaving group ability in the concerted homolytic substitution reactions involving the radical species Silyl (*SiH₃), Germynyl (*GeH₃) and Stannyl (*SnH₃) and disilane (H₃Si–SiH₃), digermene (H₃Ge–GeH₃), distannane (H₃Sn–SnH₃), silylgermane (H₃Si–GeH₃), silylstannane (H₃Si–SnH₃) and germynylstannane (H₃Ge–SnH₃). The location of the transition state struc-

tures in the potential energy surface for the backside substitution mechanism was performed at the MP2 level of theory. All calculations were done using the Stuttgart’s pseudopotentials [17] with their corresponding basis set which, however, was augmented with diffuse functions. The exponents for the functions of s and p symmetry were taken as one half of the smallest exponent of the Stuttgart basis set, and the exponent of the d-symmetry function was taken as the smallest one of the DZVP [18] basis set. The resulting basis set will be denoted as SDDALLD hereafter. The calculation of the nucleofugality index itself was performed by using electron and spin densities obtained at the B3LYP/SDDALLD//MP2/SDDALLD level.

The spin potentials μ_S^+ and μ_S^- needed to evaluate the spin hardness η_{SS}^0 were calculated using the finite difference formulas proposed by Galvan et al. [10,11], namely:

$$\mu_S^+ \approx \frac{\epsilon_L^\alpha(M) - \epsilon_H^\beta(M)}{2} \quad \text{and} \quad \mu_S^- \approx \frac{\epsilon_H^\alpha(M') - \epsilon_L^\beta(M')}{2}; \quad (5)$$

in terms of the one-electron energies of the HOMO and LUMO orbitals for the system in the lower (M) and upper (M') spin multiplicities, respectively. The spin-hardness (η_{SS}^0) can be calculated from the spin potentials as follows:

$$\eta_{SS}^0 = \frac{\mu_S^- - \mu_S^+}{2}. \quad (6)$$

With the μ_S^+ and η_{SS}^0 quantities at hand, the global spin philicity ω_S^+ is readily obtained from Eq. (2), and the condensed to atom counterpart may be projected using the spin Fukui function $f_{SS}^+(\mathbf{r})$ in the direction of increasing spin number (+) as shown in Eq. (3). This spin Fukui function can be computed using the approximations proposed by Galvan et al. [9]:

$$f_{SS}^+(\mathbf{r}) \approx \frac{1}{2} [|\varphi_L^\alpha(\mathbf{r})|^2 + |\varphi_H^\beta(\mathbf{r})|^2], \quad (7)$$

$\varphi_L^\alpha(\mathbf{r})$ and $\varphi_H^\beta(\mathbf{r})$ are the α and β LUMO and HOMO spin-orbitals, respectively. Finally, the condensed to atom k quantity $f_{SS,k}^+(k)$ needed to get the regional spin philicity $\omega_{S,k}^+$ is obtained by an integration method described elsewhere [19,20]. The homofugality index v^* is then obtained according to Eq. (4).

The prediction of the quality of leaving groups was formerly introduced by Ayers et al. [21] by means of a universal scale describing the electro and nucleofugality concepts within a spin restricted model. These authors successfully described the leaving group ability of a series of organic fragments present in nucleophilic substitution and elimination reactions. In this sense, the present contribution closes the complete description of leaving group scales by incorporating radical processes described in the frame of the spin polarized density functional theory.

3. Results and discussion

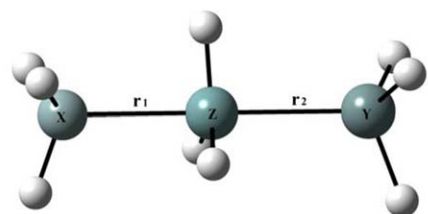
The concerted homolytic substitution by silyl radical at the silicon atom of disilane as well as those involving the

germyl radical with digermene and the stannyl radical with distannane have been studied at high ab initio levels by Schiesser et al. [6]. These authors report that both the frontside and backside attacks at the heteroatom may be operative in these processes. We relay on the results of these authors to accordingly select the simplest backside attack at the heteroatom to analyze the performance of our homofugality index to describe the reactivity towards S_H2 reactions. The general geometric arrangement is depicted in Fig. 1. Table 1 summarizes the results of the calculations performed on 36 combinations that include degenerate and nondegenerate reactions. Our aim is to incorporate a sufficient number of cases to guarantee that the departure of the radical LG's $\cdot\text{CH}_3$, $\cdot\text{SiH}_3$, $\cdot\text{GeH}_3$ and $\cdot\text{SnH}_3$ takes place in comparable conditions of bond forming processes, so that the computed energy barriers contain mostly information about the homolytic scission of the A-LG bond shown in Eq. (1). Therefore the data in Table 1 may be grouped into three series of twelve possible reactions in each case.

Series A considers the first 12 reactions shown in Table 1. In these processes, the attacking radical is $\cdot\text{SiH}_3$ and the bond forming process involves the, Si-Si, Si-Ge and Si-Sn pairs. The set of leaving radicals are $\cdot\text{CH}_3$, $\cdot\text{SiH}_3$, $\cdot\text{GeH}_3$ and $\cdot\text{SnH}_3$ in each subseries. It may be seen that in all cases, the energy barriers for the concerted S_H2 processes show an inverse relationship with the homofugality index: low barriers are consistently related to high values of homofugality of the departing radical. The same pattern is obtained for

series B and C, for which the attacking radicals are $\cdot\text{GeH}_3$ and $\cdot\text{SnH}_3$, respectively. Note that in all three series, the energy barriers associated with reactions involving bond breaking between a carbon atom and a heteroatom are consistently predicted to display the highest values in all the three series, together with the lowest values of homofugality index for the $\cdot\text{CH}_3$ radical. This result is in agreement with previous findings that suggest that intermolecular S_H2 processes involving the methyl radical are rarely observed [1,6]. A summary of the results obtained is depicted in Figs. 2-4. The general reactivity trend in terms of homofugality: $\cdot\text{CH}_3 < \cdot\text{SiH}_3 < \cdot\text{GeH}_3 < \cdot\text{SnH}_3$ that almost parallel the reactivity pattern established on the basis of the calculated energy barriers evaluated in this work is that observed for series C where the attacking radical is $\cdot\text{SnH}_3$ (see Fig. 4). For series A and B, the trends predicted from the energy barriers is roughly reproduced, the only difference being the relative order for Ge and Sn (see Figs. 2 and 3).

The relative order of Ge and Sn may be further explored by comparing the homofugality and bond order (BO) profiles along the IRC coordinate, using a procedure recently proposed [22]. These profiles, depicted in Fig. 5 may give relevant information about the bond forming/braking processes in these radical displacement reactions. For the identity reaction $\cdot\text{SiH}_3 + \text{SiH}_3\text{-SiH}_3$ (not shown in Fig. 5) the analysis is straightforward. As expected, both the homofugality index and the bond order profiles corresponding to bond making and bond breaking intersect at the transition state, with a pattern that exactly matches that found by



a

Z			
Y=X		r ₁ = r ₂	
	Si	Ge	Sn
Si	2.483	2.596	2.758
Ge	2.592	2.693	2.844
Sn	2.817	2.907	3.047

b

		Z					
		Si		Ge		Sn	
X	Y	r ₁	r ₂	r ₁	r ₂	r ₁	r ₂
Si	C	2.412	2.208	2.525	2.287	2.714	2.418
Si	Ge	2.547	2.540	2.652	2.648	2.805	2.805
Si	Sn	2.603	2.725	2.698	2.825	2.838	2.980
Ge	C	2.496	2.235	2.608	2.314	2.784	2.434
Ge	Sn	2.656	2.760	2.747	2.855	2.897	3.000
Sn	C	2.688	2.275	2.790	2.346	2.965	2.457

Fig. 1. Optimized structures of the backside transition states located at the MP2/SDDALLD level of theory for: (a) degenerate and (b) non degenerate homolytic substitution reactions: $\cdot\text{XH}_3 + \text{H}_3\text{Z-YH}_3$, X = Si, Ge, Sn; Z = Si, Ge, Sn; Y = C, Si, Ge, Sn. Bond distances in Å.

Table 1

Energy barriers ΔE^\ddagger , the spin-philicity, ω_S^+ , spin Fukui function f_{SS}^+ (LG) and homofugality index, ν^+ (LG), of the leaving group (LG), values calculated at the backside transition state structure for some degenerate and non degenerate homolytic substitution reactions^a

Reaction	LG	ΔE^\ddagger	ω_S^+	f_{SS}^+ (LG)	ν^+
$\cdot\text{SiH}_3 + \text{SiH}_3\text{-CH}_3$	$\cdot\text{CH}_3$	32.00	11.96	-0.07	-0.88
$\cdot\text{SiH}_3 + \text{SiH}_3\text{-SiH}_3$	$\cdot\text{SiH}_3$	17.14	10.97	0.39	4.23
$\cdot\text{SiH}_3 + \text{SiH}_3\text{-GeH}_3$	$\cdot\text{GeH}_3$	14.78	10.84	0.60	6.48
$\cdot\text{SiH}_3 + \text{SiH}_3\text{-SnH}_3$	$\cdot\text{SnH}_3$	13.15	9.68	0.54	5.22
$\cdot\text{SiH}_3 + \text{GeH}_3\text{-CH}_3$	$\cdot\text{CH}_3$	26.50	9.50	0.04	0.38
$\cdot\text{SiH}_3 + \text{GeH}_3\text{-SiH}_3$	$\cdot\text{SiH}_3$	17.14	8.93	0.25	2.28
$\cdot\text{SiH}_3 + \text{GeH}_3\text{-GeH}_3$	$\cdot\text{GeH}_3$	14.49	8.81	0.40	3.51
$\cdot\text{SiH}_3 + \text{GeH}_3\text{-SnH}_3$	$\cdot\text{SnH}_3$	13.26	8.09	0.37	3.01
$\cdot\text{SiH}_3 + \text{SnH}_3\text{-CH}_3$	$\cdot\text{CH}_3$	22.17	9.54	0.08	0.78
$\cdot\text{SiH}_3 + \text{SnH}_3\text{-SiH}_3$	$\cdot\text{SiH}_3$	14.23	9.07	0.26	2.35
$\cdot\text{SiH}_3 + \text{SnH}_3\text{-GeH}_3$	$\cdot\text{GeH}_3$	12.49	8.89	0.37	3.31
$\cdot\text{SiH}_3 + \text{SnH}_3\text{-SnH}_3$	$\cdot\text{SnH}_3$	11.20	8.20	0.39	3.19
$\cdot\text{GeH}_3 + \text{SiH}_3\text{-CH}_3$	$\cdot\text{CH}_3$	35.38	11.54	-0.03	-0.39
$\cdot\text{GeH}_3 + \text{SiH}_3\text{-SiH}_3$	$\cdot\text{SiH}_3$	19.65	10.84	0.19	2.11
$\cdot\text{GeH}_3 + \text{SiH}_3\text{-GeH}_3$	$\cdot\text{GeH}_3$	16.67	10.53	0.50	5.26
$\cdot\text{GeH}_3 + \text{SiH}_3\text{-SnH}_3$	$\cdot\text{SnH}_3$	14.39	9.55	0.44	4.22
$\cdot\text{GeH}_3 + \text{GeH}_3\text{-CH}_3$	$\cdot\text{CH}_3$	29.33	9.16	0.04	0.34
$\cdot\text{GeH}_3 + \text{GeH}_3\text{-SiH}_3$	$\cdot\text{SiH}_3$	19.26	8.81	0.17	1.47
$\cdot\text{GeH}_3 + \text{GeH}_3\text{-GeH}_3$	$\cdot\text{GeH}_3$	16.32	8.72	0.32	2.83
$\cdot\text{GeH}_3 + \text{GeH}_3\text{-SnH}_3$	$\cdot\text{SnH}_3$	14.58	8.10	0.34	2.78
$\cdot\text{GeH}_3 + \text{SnH}_3\text{-CH}_3$	$\cdot\text{CH}_3$	23.98	9.18	0.08	0.75
$\cdot\text{GeH}_3 + \text{SnH}_3\text{-SiH}_3$	$\cdot\text{SiH}_3$	15.50	8.89	0.18	1.64
$\cdot\text{GeH}_3 + \text{SnH}_3\text{-GeH}_3$	$\cdot\text{GeH}_3$	13.99	8.87	0.27	2.43
$\cdot\text{GeH}_3 + \text{SnH}_3\text{-SnH}_3$	$\cdot\text{SnH}_3$	12.18	8.22	0.33	2.70
$\cdot\text{SnH}_3 + \text{SiH}_3\text{-CH}_3$	$\cdot\text{CH}_3$	39.96	9.92	-0.01	-0.09
$\cdot\text{SnH}_3 + \text{SiH}_3\text{-SiH}_3$	$\cdot\text{SiH}_3$	23.90	9.68	0.14	1.32
$\cdot\text{SnH}_3 + \text{SiH}_3\text{-GeH}_3$	$\cdot\text{GeH}_3$	20.28	9.55	0.31	2.95
$\cdot\text{SnH}_3 + \text{SiH}_3\text{-SnH}_3$	$\cdot\text{SnH}_3$	17.44	9.18	0.34	3.17
$\cdot\text{SnH}_3 + \text{GeH}_3\text{-CH}_3$	$\cdot\text{CH}_3$	32.34	8.25	0.05	0.42
$\cdot\text{SnH}_3 + \text{GeH}_3\text{-SiH}_3$	$\cdot\text{SiH}_3$	22.16	8.09	0.12	1.01
$\cdot\text{SnH}_3 + \text{GeH}_3\text{-GeH}_3$	$\cdot\text{GeH}_3$	18.71	8.10	0.21	1.71
$\cdot\text{SnH}_3 + \text{GeH}_3\text{-SnH}_3$	$\cdot\text{SnH}_3$	16.71	7.80	0.24	1.88
$\cdot\text{SnH}_3 + \text{SnH}_3\text{-CH}_3$	$\cdot\text{CH}_3$	26.30	8.41	0.10	0.84
$\cdot\text{SnH}_3 + \text{SnH}_3\text{-SiH}_3$	$\cdot\text{SiH}_3$	17.82	8.20	0.15	1.25
$\cdot\text{SnH}_3 + \text{SnH}_3\text{-GeH}_3$	$\cdot\text{GeH}_3$	15.79	8.22	0.17	1.43
$\cdot\text{SnH}_3 + \text{SnH}_3\text{-SnH}_3$	$\cdot\text{SnH}_3$	13.94	7.96	0.25	1.98

^a Values of ΔE^\ddagger in kcal/mol at MP2/SDDALLD level of theory; ω_S^+ and ν^+ values are given in eV units. The indexes ω_S^+ , f_{SS}^+ and ν^+ are calculated at MP2/SDDALLD//B3LYP/SDDALLD level of theory.

Chattaraj and Roy for the analogous termoneutral S_N2 reaction [22]. For the non degenerate reactions involving the departure of $\cdot\text{GeH}_3$ and $\cdot\text{SnH}_3$ in comparable conditions of bond forming processes the crossing point of the BO profiles occurs almost at the TS position, thereby suggesting that the bond breaking processes involving the $\cdot\text{GeH}_3$ and $\cdot\text{SnH}_3$ radicals are very similar. Note that the intersection of the homofugality profiles appear shifted right to the TS, thereby suggesting that the departure of the LG takes place through an early TS.

However, a definitive answer to settle the reactivity order predicted from the homofugality index demands the experimental rate coefficients for these processes, together with a complete analysis of both reaction channels

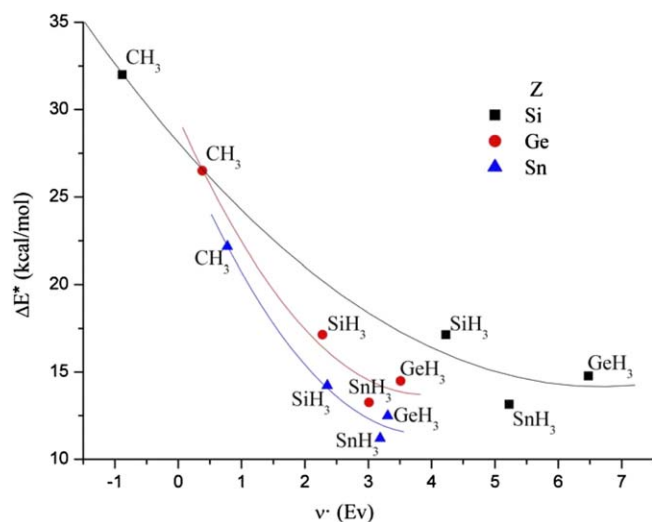


Fig. 2. Comparison between energy barriers ΔE^\ddagger and the homofugality index ν^+ at the transition state for the backside homolytic substitution reactions between $\cdot\text{SiH}_3$ and $\text{H}_3\text{Z-YH}_3$. Y = C, Si, Ge, Sn; Z = Si, Ge, Sn.

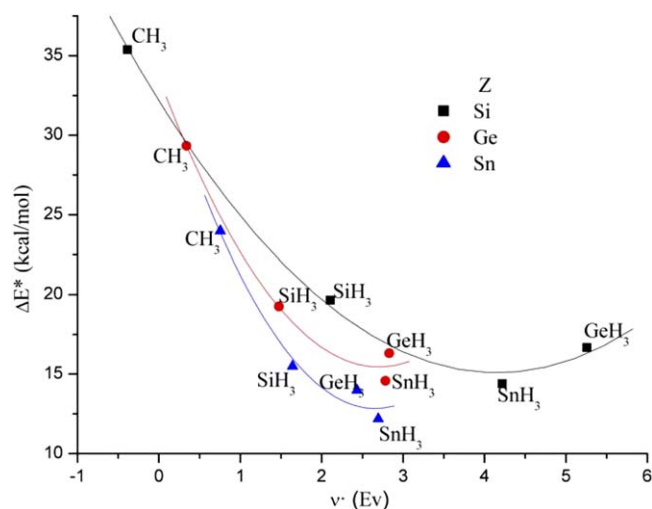


Fig. 3. Comparison between energy barriers ΔE^\ddagger and the homofugality index ν^+ at the transition state for the backside homolytic substitution reactions between $\cdot\text{GeH}_3$ and $\text{H}_3\text{Z-YH}_3$. Y = C, Si, Ge, Sn; Z = Si, Ge, Sn.

which at present is beyond the scope of this work. However, based on the calculated energy barriers for the backside mechanism, it seems that under conditions of comparable bond forming processes, the homofugality index qualitatively assesses the reactivity order predicted for these systems.

The origin of the reactivity order established on the basis of the homofugality index may be further discussed by giving a closer look at Table 1. Therein we have compiled in columns 4th and 5th the values of the global spin philicity ω_S^+ and the spin Fukui function in the direction of increasing multiplicity f_{SS}^+ condensed at the leaving group LG. The global index ω_S^+ measures the philicity of the system to undergo spin polarization [12]. Note that in

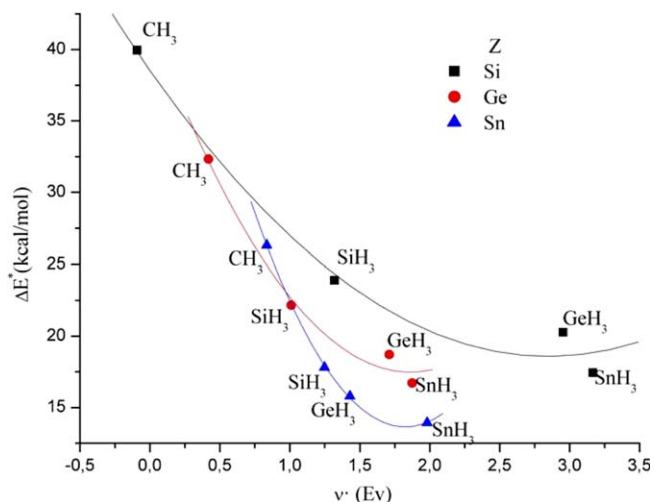


Fig. 4. Comparison between energy barriers ΔE^\ddagger and the homofugality index ν^\ddagger at the transition state for the backside homolytic substitution reactions between $\cdot\text{SnH}_3$ and $\text{H}_3\text{Z}-\text{YH}_3$. $\text{Y} = \text{C}, \text{Si}, \text{Ge}, \text{Sn}$; $\text{Z} = \text{Si}, \text{Ge}, \text{Sn}$.

all cases, the highest global spin philicity values quoted in Table 1 correspond to those transition state structures that bear the $\cdot\text{CH}_3$ radical as the leaving group. For the remaining cases where the LG involves the heteroatom $\text{Z} = \text{Si}, \text{Ge}, \text{Sn}$, the global spin philicity show a decreasing pattern from Si to Sn, yet the differences in ω_S^+ values within the sub series that shares a common attacking radical is relatively small. However, the values of the spin Fukui function in the direction of increasing multiplicity f_{SS}^+ condensed at the leaving group LG discriminate better within the different sub series. As a matter of fact, the low homofugality pattern displayed by the transition state structures bearing the $\cdot\text{CH}_3$ fragment as LG's may be strictly traced to the low values of the spin Fukui function f_{SS}^+ condensed on the CH_3 group at the transition state. For the remaining cases, the f_{SS}^+ values condensed to groups SiH_3 , GeH_3 and SnH_3 show in general an increasing pattern from Si to Sn, thereby determining the homofugality

order observed for these systems. If we remember that according to the spin polarized density functional theory, the generalized Fukui function $f_{\text{SS}}^+(\mathbf{r})$ in the direction of increasing or decreasing multiplicity is a normalized spin softness [14] and as such it may be viewed as a measure of the 'polarizability' of the spin density, we may conclude that the reactivity order obtained from the homofugality analysis is mainly driven by the regional spin softness which increases in the order $\text{C} < \text{Si} < \text{Ge} \sim \text{Sn}$. The parallel with the polar $\text{S}_{\text{N}}2$ process is remarkable if we consider that the observed leaving group order in the halogen series is $\text{Cl} < \text{Br} < \text{I}$, a relative order that is also dictated by the chemical softness defined in the unrestricted density functional theory. This 'electronic' softness is also a measure of the polarizability of the electronic cloud and plays an important role in a parent concept: the nucleofugality, which is related to the leaving group ability in heterolytic bond cleavage reactions [23]. In the process of the review of this Letter, a referee called our attention on a recent work by Geerlings et al. [24] who presented a spin restricted study on the functional groups $-\text{XY}_3$ that included the XH_3 series ($\text{X} = \text{C}, \text{Si}, \text{Ge}, \text{Sn}$). It is interesting to note that the spin restricted electrophilicity index increases in the order $\text{CH}_3 < \text{SiH}_3 < \text{GeH}_3 < \text{SnH}_3$. If we consider that the LG departs with one bonding electron after the homolytic scission, its electrophilicity may also be an important factor on which the homofugality depends.

4. Concluding remarks

A new descriptor of reactivity, the homofugality index, has been introduced and tested for a series of $\text{S}_{\text{H}}2$ processes involving organometallic systems. The homofugality index encompasses the global spin philicity of the system projected into the leaving group moiety using the generalized spin Fukui function. The homofugality evaluated at the transition state of the backside pathway for intermolecular $\text{S}_{\text{H}}2$ processes involving Methyl, Silyl, Germyl and Stannyl radicals assesses well the observed order of reactivity

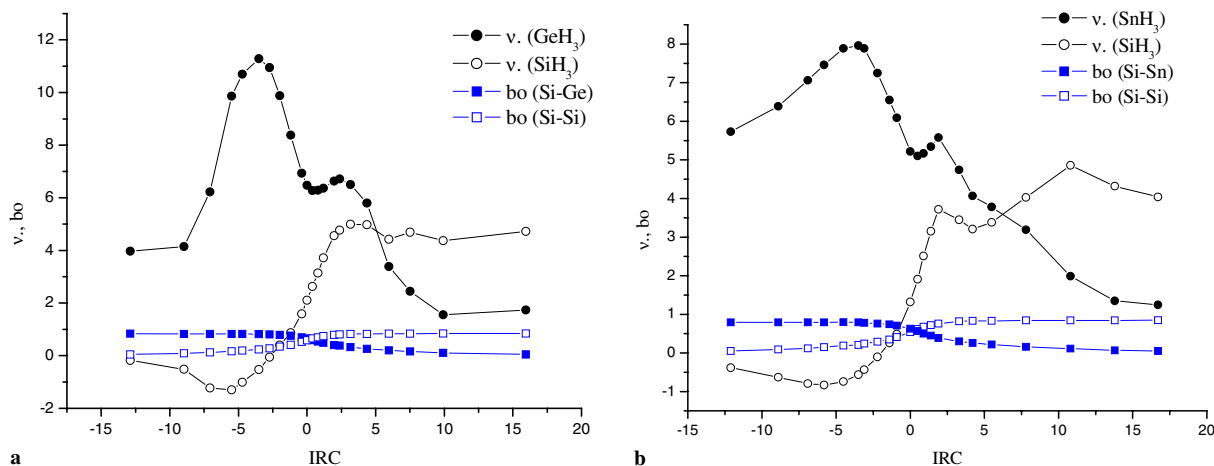


Fig. 5. Homofugality and bond order profiles along the IRC for: (a) $\cdot\text{SiH}_3 + \text{H}_3\text{Si}-\text{GeH}_3$ and (b) $\cdot\text{SiH}_3 + \text{H}_3\text{Si}-\text{SnH}_3$ reactions.

established for these systems from highly accurate calculations. The homofugality order is driven by the spin Fukui function describing the regional spin softness at the LG moiety, in a form which is reminiscent of the nucleofugality order of the halogen series observed in the parent S_N2 polar process which also depends on the regional electronic softness of the leaving group.

Acknowledgements

This work has received financial support from Fondecyt, project 1050523, the Millennium Nucleus for Applied Quantum Mechanics and Computational Chemistry, Grant P02-004-F and Universidad Andrés Bello, Grant UNAB-DI-08-05/I. D.G. is grateful to Universidad Andrés Bello for a graduate fellowship. R.C. acknowledges Fundación Bancaixa-UJI for financial support during his research stay at UJI, Castellón, Spain.

References

- [1] J.C. Walton, *Acc. Chem. Res.* 31 (1998) 99.
- [2] K.U. Ingold, B.P. Roberts, *Free Radical Substitution Reactions*, Wiley Interscience, New York, 1971.
- [3] C.H. Schiesser, L.M. Wild, *Tetrahedron* 52 (1996) 13265.
- [4] H. Fischer (Ed.), *Numerical Data and Functional Relationships in Science and Technology*, Landolt-Bornstein Series, vol. II/18, Springer, Berlin, 1994.
- [5] M. Newcomb, R.M. Sánchez, J. Kaplan, *J. Am. Chem. Soc.* 109 (1987) 1195.
- [6] S.M. Horvat, C.H. Schiesser, L.M. Wild, *Organometallics* 19 (2000) 1239.
- [7] C.H. Schiesser, L.M. Wild, *J. Org. Chem.* 63 (1998) 670.
- [8] C.H. Schiesser, L.M. Wild, *J. Org. Chem.* 64 (1999) 1131.
- [9] M. Galván, A. Vela, J.L. Gázquez, *J. Phys. Chem.* 92 (1988) 6470.
- [10] M. Galván, R. Vargas, *J. Phys. Chem.* 96 (1992) 1625.
- [11] R. Vargas, M. Galván, A. Vela, *J. Phys. Chem. A* 102 (1998) 3134.
- [12] P. Pérez, J. Andres, V.S. Safont, O. Tapia, R. Contreras, *J. Phys. Chem. A* 106 (2002) 5353.
- [13] F. De Proft, S. Fias, C. Van Alsenoy, P. Geerlings, *J. Phys. Chem. A* 109 (2005) 6335.
- [14] D. Guerra, R. Contreras, P. Pérez, P. Fuentealba, *Chem. Phys. Lett.* 419 (2006) 37.
- [15] J. Olah, F. De Proft, T. Veszpremi, P. Geerlings, *J. Phys. Chem. A* 108 (2004) 490.
- [16] J. Olah, T. Veszpremi, M.T. Nguyen, *Chem. Phys. Lett.* 401 (2005) 337.
- [17] A. Bergner, M. Dolg, W. Kuechle, H. Stoll, H. Preuss, *Mol. Phys.* 80 (1993) 1431.
- [18] N. Godbout, D.R. Salahub, J. Andzelm, E. Wimmer, *Can. J. Chem.* 70 (1992) 560.
- [19] R. Contreras, P. Fuentealba, M. Galván, P. Pérez, *Chem. Phys. Lett.* 304 (1999) 405.
- [20] P. Fuentealba, P. Pérez, R. Contreras, *J. Chem. Phys.* 113 (2000) 2544.
- [21] P.W. Ayers, J.S.M. Anderson, J.I. Rodriguez, Z. Jawed, *Phys. Chem. Chem. Phys.* 7 (2005) 1918.
- [22] P.K. Chattaraj, D.R. Roy, *J. Phys. Chem. A* 109 (2005) 3771.
- [23] C.J.M. Stirling, *Acc. Chem. Res.* 12 (1979) 198.
- [24] K.T. Giju, F. De Proft, P. Geerlings, *J. Phys. Chem. A* 109 (2005) 2925.